

## Ultrafast dynamics and carrier-envelope phase sensitivity of multiphoton photoemission from metal surfaces

P. DOMBI\*†¶, F. KRAUSZ‡§ and G. FARKAS¶

†Institut für Photonik, Technische Universität Wien,  
Gusshausst. 27, A-1040 Wien, Austria

‡Max-Planck-Institut für Quantenoptik, Hans-Kopfermann-Str. 1,  
D-85748 Garching, Germany

§Ludwig-Maximilians-Universität, Am Coulombwall 1,  
D-85748 Garching, Germany

¶Research Institute for Solid State Physics and Optics,  
PO Box 49, H-1525, Budapest, Hungary

*(Received 22 March 2005; in final form 20 April 2005)*

Subcycle dynamics of multiphoton-induced photoelectron emission from metal surfaces is analysed using a simple phenomenological model to assess optimum conditions for direct carrier-envelope phase measurement. To gain further insight femtosecond time-resolved measurements were carried out on a polycrystalline gold surface with ultrashort laser pulses to explain the recently found, unexpectedly low carrier-envelope phase dependence of the photoemission process in this particular case. In the higher-order interferometric autocorrelation distribution additional short side wings appeared suggesting that ultrafast dynamics of hot electrons reduce the carrier-envelope phase dependence of the photoemission electron yield produced by few-cycle laser pulses. Other metals can be investigated with this simple and fast method to pave the way towards the construction of a solid-state-based, direct carrier-envelope phase detector.

### 1. Introduction

The generation of intense, few-cycle Ti:sapphire laser pulses opened up new possibilities for experimental studies of the characteristics of highly nonlinear interactions [1]. Attosecond pulse generation has been one of the most spectacular benefits of few-cycle pulse-driven interactions so far (see [2] and references therein). Attosecond metrology with these pulses requires precise control and measurement of the carrier-envelope (CE) phase of intense sub-10-fs laser pulses, but currently used, optically and electronically complicated methods based on the so-called  $f$ -to- $2f$  interferometry do not necessarily fulfil these requirements [3].

Multiphoton-induced surface photoelectron emission (MSPE) using CE phase-controlled pulses has recently become of interest due to its potential ability to

---

\*Corresponding author. Email: [dombi@szfki.hu](mailto:dombi@szfki.hu)

overcome the above limitations [3–5]. Moreover, it could find novel applications related to ultrafast, keV photoelectron sources and detection and surface science [6, 7]. The femtosecond dynamics of MSPE has been studied extensively in the last decade by experts in the latter field, resulting in sophisticated, temporally, spectrally and spatially resolved electron emission studies (see [8, 9] and references therein). Related characterization methods, such as photoelectron emission microscopy (PEEM) were also upgraded for use with femtosecond lasers [10, 11] and femtosecond dynamics of the electronic states of surface adsorbates can also be studied with time-resolved two-photon photoemission methods [12]. In spite of these recent developments in basic research and methodology, studies in the few-cycle laser pulse length domain are scarce and thus the role of the CE phase in the photoemission process is not well understood, in spite of the enormous potential of this field. Such an understanding would pave the way towards surface attosecond science since in standard attosecond XUV/infrared pump-probe-like setups (that have been employed for the investigation of gas-phase interactions) in which one of the interacting fields is a CE phase-controlled infrared pulse [2].

In this paper we present theoretical and experimental investigations with the aim of gaining insight into the subcycle and femtosecond dynamics of MSPE from metal surfaces using few-cycle Ti:sapphire laser pulses. A simple, phenomenological model is employed, the basics of which were described recently [3]. We develop it further to enable quantitative estimates for the photocurrent as a function of the CE phase. Our results can then be compared to those delivered by a sophisticated simulation using the jellium model of metals and density functional methods [4]. We carry out femtosecond time-resolved studies of the emission process with an inexpensive and compact electron detector tube to assess potential additional effects not taken into account by the model. Our study sheds light on the possible origin of the recently found, unexpectedly low experimental dependence of laser-induced multiphoton electron emission on the CE phase [3, 5].

## 2. Model for carrier-envelope phase-sensitive photoelectron emission

To gain a deeper understanding of CE phase-sensitive MSPE, we adapt the so-called three-step semiclassical model of gas-phase high harmonic generation [13] to surface photoemission. In Corkum's model the electron ionized by the field of a laser pulse is assumed to be "born" in the continuum with zero initial velocity after tunnelling through the potential barrier distorted by the laser field. Thereafter it is treated as a free particle and its trajectory is examined in the potential of the laser field only. Under certain conditions the wave packet returns to the parent ion and the subsequent recombination results in the emission of high-harmonic photons. This simple picture results in remarkably accurate quantitative predictions and forms the basis for a rigorous quantum mechanical treatment of the process [14]. Obviously, the time of birth, the instant of the recombination, and consequently the temporal and spectral characteristics of the XUV emission are also influenced by the CE phase of the laser pulse provided that the generating pulses have few-cycle duration.

The model can be adapted to MSPE to account for CE phase effects. The first step corresponds to instantaneous electron emission as a result of which a free electron is “born” somewhere near the metal surface. We assume that the probability of the emission is proportional to  $A(t)^{2n}$ , where  $A(t)$  is the envelope of a laser pulse the  $E$ -field of which is described by  $E(t) = A(t) \cos(\omega_0 t + \varphi_{CE})$ . (Here  $\omega_0$  is the carrier frequency and  $\varphi_{CE}$  denotes the carrier-envelope phase.) The order of nonlinearity of the process is denoted by  $n$ , and the  $A(t)^{2n}$ -assumption for the emission probability is in accordance with the perturbative nature of MSPE and well-known, justified intensity dependence laws.

The second step in our treatment is to determine the motion of the electron near the surface. Trajectories are assumed to be influenced only by the laser field and the mirror charge potential. The latter effect appears to be negligible according to numerical simulations. Depending on the actual CE phase of the pulse the field evolution will push the electron back to the surface either immediately upon emission (figure 1; the hypothetical thin dash-dotted line is in the  $z < 0$  region, which means an assumption of no emission taking place) or after performing a wiggle in the laser field.

It is also possible that the electron is able to escape (figure 1, thick dash-dotted line). As an example, figure 1 shows calculations for an electron that is released exactly at the peak of the intensity envelope of the pulse. However, to gain

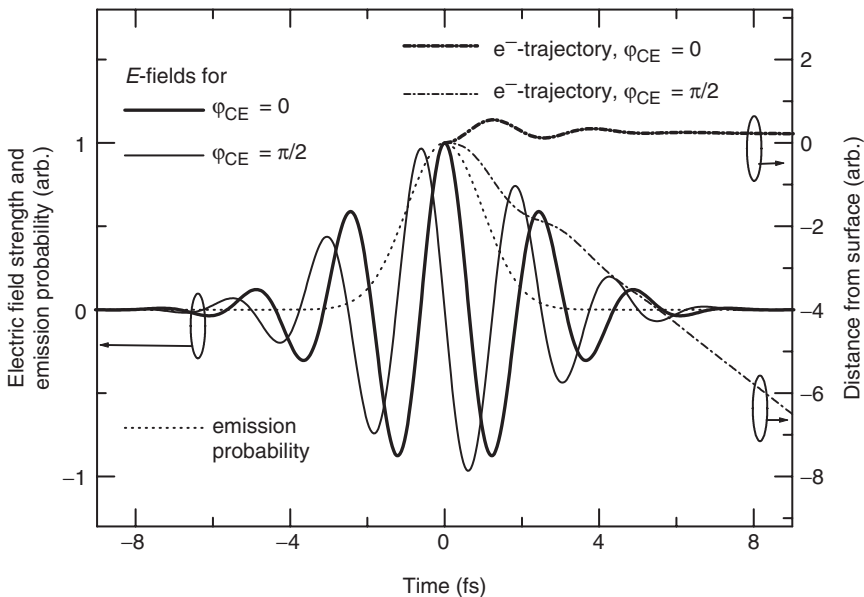


Figure 1. Electric field evolution of a transform-limited *cosine*- (thick solid line) and a *sine-pulse* (thin solid line) in the case of a Gaussian 4 fs (intensity) envelope. The dotted line shows the photoemission probability assuming a third-order process. The dash-dotted lines depict classical trajectories of the electrons that are emitted with the highest probability at the peak of the pulse envelope. Since on the right axis the  $z < 0$  region indicates the metal bulk, we assumed that when the trajectory hits this region no electron emission takes place.

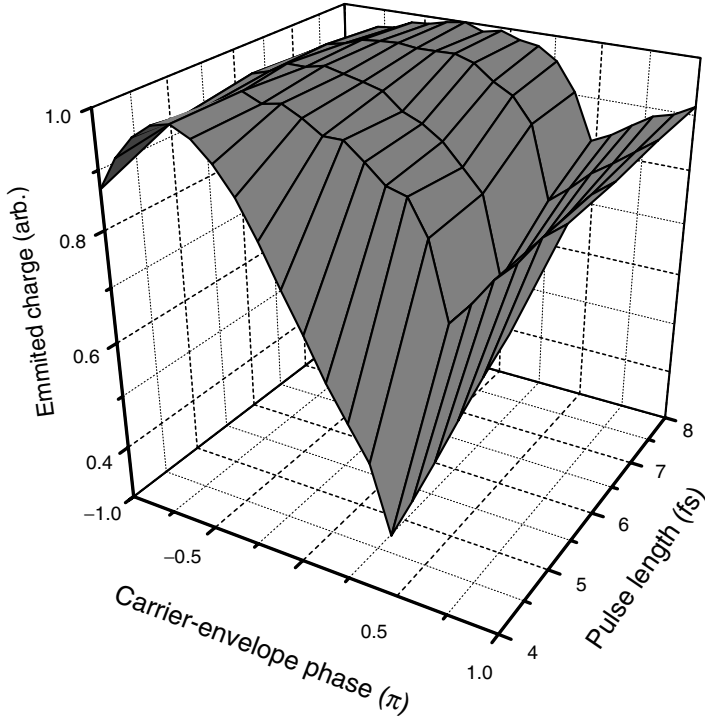


Figure 2. Photoelectron yield resulting from a simple model of CE phase-sensitive MSPE as a function of the CE phase and the pulse length. The figure is directly comparable to figure 2 of [3].

quantitative results other possible emission times ( $t_i$ ) have to be taken into account. For each potential emission instant the favourable range of CE phases can be determined in which the electron can escape. These ranges can then be overlapped with their corresponding weights of  $A(t_i)^{2n}$  resulting in a histogram-like distribution of electron release probabilities as a function of the CE phase.

Following this method the CE phase dependence of the electron yield was estimated as a function of the pulse length. Results are depicted in figure 2 (for this a Gaussian, transform-limited pulse and  $n=3$  were assumed, the latter corresponding to a gold surface illuminated by Ti:sapphire laser pulses).

The surface plot gained in such a way can be compared directly to the one resulting from a sophisticated simulation of the process involving the jellium model of metals and density functional methods [3, 4] as depicted in figure 2 of [3]. The agreement between the two curves computed with radically different methods is remarkable. Both the value of the CE phase at which maximum electron yield can be observed ( $\varphi_{\text{CE,Max}} = -\pi/4$ ) and the modulation depth of the curves for different pulse lengths are also correct to within 10%. Bigger deviations than this can only be observed as moving away from the few-cycle case.

In a similar way the CE phase dependence of MSPE can be examined with the order of nonlinearity of the emission process as a parameter. In figure 3 the cases

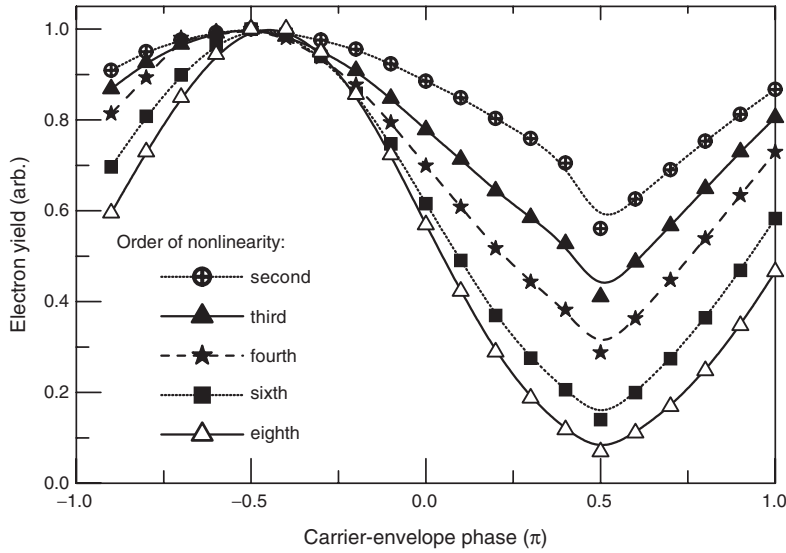


Figure 3. Photoelectron yield of MSPE induced by a 4 fs Gaussian pulse for metal surfaces with different work functions resulting in second-, third-, and fourth-order nonlinearities.

$n=2, 3, 4, 6$  and  $8$  are depicted. In this way one can estimate the effect of using metals of different work functions at the Ti:sapphire wavelength ( $n=2, 3, 4$ ). Higher order nonlinearities also come into play when it comes to CE phase detection of the planned ultrashort-pulsed chirped-pulse-amplified (CPA) lasers operating in the infrared (to be realized by broadband optical parametric amplification). This wavelength shift with respect to standard Ti:sapphire lasers brings huge benefits to high-harmonic generation and attosecond applications because of the  $\lambda^2$ -scaling of the ponderomotive potential and thus the cut-off frequency of high-harmonic generation. An additional benefit is that for these longer wavelengths the nonlinearity of the photoemission process is much higher and therefore chances of measuring the carrier-envelope phase by MSPE (or any kind of nonlinear effect [15]) increase enormously. The curves belonging to  $n=6$  and  $8$  illustrate this effect. Taking the work function of gold and a  $2\ \mu\text{m}$  optical parametric CPA laser wavelength, one would expect an eighth-order nonlinearity. This increases the CE phase-dependent modulation drastically, as seen in figure 3.

### 3. Experiments

The next task is to detect any kind of ultrafast characteristic in the photoemission to assess potential additional effects causing the previously observed low CE phase sensitivity of the electron yield [3, 5]. These effects are taken into account neither by the model in [4] nor by the one in the previous section. Experimental findings on the ultrafast dynamics of MSPE would eventually allow further refinement of the model.

In the perturbative regime the photoemission process can be characterized by measuring the intensity and polarization dependences of the photocurrent. The dependence on the intensity  $j \propto I^n$  (where  $I$  denotes the laser intensity) demonstrates the  $n$ th order perturbative multiphoton character of the interaction. The polarization dependence can demonstrate that the major contribution to the emission process is delivered by the field component perpendicular to the surface. Furthermore, MSPE as an  $n$ th-order detection process, may be used together with a Michelson interferometer as an extremely sensitive,  $n$ th-order intensity or interferometric autocorrelator to carry out ultrafast time-resolved experiments on the photoemission process.

Following these considerations we used linearly polarized 0.9 mJ, 25 fs, 800 nm pulses from a chirped-pulse-amplified Ti:sapphire laser [16] and 0.3 mJ, 9.5 fs, 750 nm pulses from a subsequent hollow-fibre/chirped-mirror compressor to study these phenomena. With these pulses we induced photoemission from a 1 mm thick, polished, chemically treated and baked polycrystalline gold surface. It was placed in a sealed glass tube ( $10^{-7}$  mbar) together with the electron collecting electrode kept at  $\sim 15$  kV. The thickness of the optical window of the vacuum vessel was reduced to 1.1 mm. This amount of glass was compensated for by inserting an extra chirped mirror in the beam path. The pulses were focused at a  $\sim 80^\circ$  grazing incidence angle on the surface. From the  $W = 4.6$  eV work function value of gold and the 1.55 eV laser photon energy it follows that  $n = [W/\hbar\omega_0 + 1] = 3$  (square brackets here indicate the greatest integer smaller than the argument).

In the first experiment to confirm the order of nonlinearity of the effect (i.e. the value  $n$ ) the  $j = f(I)$  intensity dependence was measured. The laser intensity variation was limited to the  $10^{10} - 10^{12}$  W/cm<sup>2</sup> range (to avoid both the eventual space charge saturation and the tunnel effect) and was realized by Fresnel reflecting a portion of the beam off 5  $\mu$ m thin pellicle beamsplitters at different angles of incidence (and using, of course, the transmitted beam). This way we avoided any kind of additional dispersive, diffraction or pointing instability artefacts upon intensity variation that would render subsequent measurement data points incomparable. Plotting the measured MSPE current ( $j$ ) against the average monitor power of the pulse train in a log-log coordinate system, the slope of the fit curve gives the power value  $n$  (figure 4, inset).

It can be seen that in this intensity range the predicted  $j \propto I^n$  multiphoton relation holds with an  $n \sim 3$  measured slope value for both the  $\sim 25$  fs and the  $\sim 10$  fs laser pulses.

As another initial check, we also measured the polarization dependence of the photoemission. It was performed by inserting and rotating a  $\lambda/2$  wave plate in the train of 25 fs long pulses. The polarization direction of the incident light was determined by the angle  $\theta$  between the plane of polarization of the electric vector and the normal to the plane of the cathode surface. The experimental results are presented in figure 4. The measured photocurrent  $j$  is found to depend on the perpendicular field component as theoretically predicted, i.e.  $j \propto \cos^{2n}\theta = \cos^6\theta$ , corresponding to the conditions of (vectorial) MSPE. The small deviation of the measured values from the theoretical ones may be attributed to the fact that the light was not perfectly linearly, but slightly elliptically polarized.

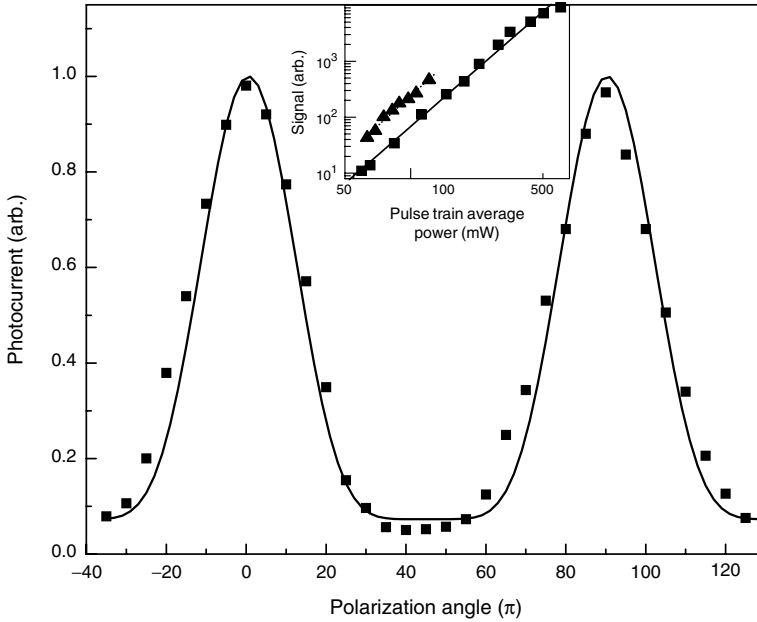


Figure 4. MSPE photocurrent as a function of the polarization angle ( $\theta$ , measured with respect to the  $E$ -field of a ‘P’-polarized beam). The fit is a  $\cos^6$  function. For the measurement  $\sim 25$  fs pulses were utilized. The inset shows the intensity dependence of the MSPE photocurrent measured with  $\sim 25$  fs long (squares) and  $\sim 10$  fs long (triangles) laser pulses plotted on a log–log scale, in arbitrary units. The slopes of the fits to the measured points correspond to orders of nonlinearity of  $2.9 \pm 0.1$ , and  $3.1 \pm 0.2$ , respectively. The relative position of the two data sets is not meaningful, since different focusing geometries were used.

The third and most important part of our experiment was devoted to the investigation of the temporal behaviour of MSPE. We carried out a measurement using the gold cathode at the exit of a Michelson interferometer as a multiphoton ( $n=3$ ) detector at grazing incidence. Using the  $\sim 10$  fs laser pulses we have taken interferometric autocorrelation curves. A typical distribution can be seen in figure 5 where the insets show the conventional second harmonic autocorrelation curve of the laser pulse and its spectrum for reference. Using the data presented in the insets the polynomial spectral phase of the pulse could be roughly reconstructed by fitting the coefficients of second-, third- and fourth-order phase terms. The contours of the autocorrelation trace that was calculated using the measured spectral intensity and the reconstructed spectral phase data match well those of the measured second-order autocorrelation curve and indicate uncompensated higher order dispersion in the system.

However, when we measured the high order ( $n=3$ ) autocorrelation curve, we saw that it differed significantly from the reconstructed one using the pulse data acquired in the above manner (figure 5, contour traces in the main part of the figure). The  $\sim 25$  fs lengthening in both wings cannot simply be explained by uncompensated

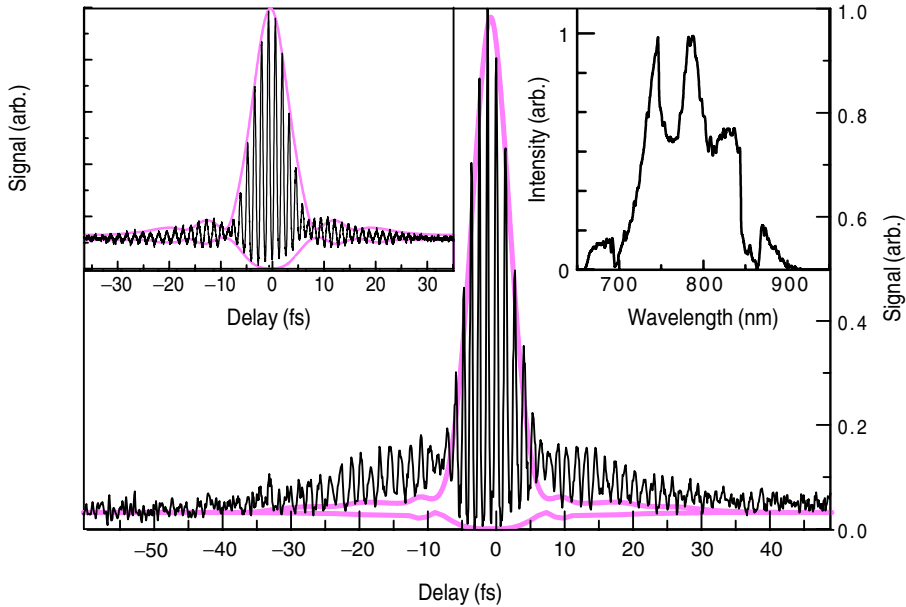


Figure 5. Measured third-order autocorrelation curve of a 9.5 fs laser pulses using the gold surface. The thick contour line corresponds to the reconstructed envelope of the third-order autocorrelation function of the pulse by fitting a polynomial spectral phase function. The left-hand-side inset shows a pulse diagnostic measurement carried out with a conventional second harmonic autocorrelator and the reconstructed envelope of the second-order autocorrelation curve using the same polynomial spectral phase function. The right-hand side inset shows the spectrum of the pulse. (The colour version of this figure is included in the online version of the journal.)

higher order dispersion in the system, but demonstrate the appearance of the decay of some of the induced energy levels of the metal target. (At long delays though, coinciding with the theoretical prediction the curves show the correct 32:1 contrast value, indicating third-order MSPE from gold.)

#### 4. Discussion

Our observations on time-resolved MSPE are in accordance with previous studies of photoemission from other types of surfaces with longer pulses and for the  $n=2$  case [17–21] and indicate ultrafast dynamics of hot electrons. It is known that ultrafast intense laser pulses may induce a laser-photon-energy separated energy level structure extending over the metallic potential well and the continuum [22, 23]. (This structure is the base of the above threshold ionization-type electron emission and of the high harmonic generation applied for the case of solids [24, 25].) The problem of ultrafast dynamic formation of a level structure spaced by  $\hbar\omega_0$  [17], furthermore the decay of the vacuum levels have been extensively investigated for the  $n=2$  case [18–21]. Autocorrelation methods were used to probe intermediate electron states and thus their lifetimes were extracted. Previous calculations and

experiments show the appearances of short and long decay times manifesting in the lengthened wings of the second-order interferometric autocorrelation distributions at excitation of metal surfaces and bulk (for  $n = 2$ ) [18–21]. The lifetime values acquired in such a way were partly confirmed by first-principles calculations, too [26].

The deconvolution procedure on the experimental correlation data is the simplest for the case of two-photon-induced transitions. However, MSPE is of particular interest for CE phase detection where a higher-order nonlinearity is desired, as pointed out above. In this case the extraction of lifetime information becomes more complicated due to the increasing number of emission channels through a set of intermediate states, therefore we can only draw qualitative conclusions from the measurements at this stage. This approach is satisfactory as long as one wants to see how the carrier-envelope phase sensitivity of the emission is affected which was the main objective of our studies.

The decoherence of these electron states on the observed time scale obviously leads to the severe loss of the sensitivity of the MSPE electron yield to the carrier-envelope phase, which is also supported by recent observations [3, 5]. Instantaneous electron emission is predicted to cause a yield modulation of as much as 50% for 5 fs pulses, whereas the observed modulation depth was well below this level. Therefore, further considerations are needed to enable us to identify which material configuration can be applied successfully for CE phase detection. The autocorrelation method described above allows us to characterize potential candidates for CE phase measurement without having to draw on the valued beamtime of CE phase-stabilized lasers. If we combine the detection system with an electron multiplier, as in our previous studies [3, 5], the output of a Ti:sapphire oscillator is enough to carry out these diagnostic measurements. Therefore, as a next step the MSPE characteristics of a single-crystal gold surface will be studied with 5 fs laser pulses. The conclusions drawn will also enable us to develop our model further.

## 5. Summary

In summary, we have presented a simplified approach to CE phase sensitive MSPE, the conclusions of which are in remarkable agreement with simulations using the jellium model of metals. We have also performed additional experiments on MSPE of gold induced by few-cycle laser pulses in order to study its characteristics in the few-cycle case to come to an understanding of the reduced CE phase sensitivity observed in recent experiments [3–5]. The intensity and polarization dependences did agree well with previous observations performed with longer pulses. Using the high-order autocorrelation curve, however, we observed temporal lengthening in the interaction process indicating ultrafast level dynamics in the femtosecond range. This explains the discrepancy between recent simulations and measurements in terms of the influence of the CE phase on the electron emission process. Since this effect strongly decreases the dependence of multiphoton processes on the carrier-envelope phase of few-cycle laser pulses, further theoretical and experimental study of the phenomenon in the few-cycle, controlled-waveform regime is necessary. This would also contribute to the understanding of sub-10-fs electron dynamics of metal surfaces

and would lead to the eventual construction of a direct, compact, low-cost and single-shot CE phase detector, particularly promising for infrared wavelengths. This would immediately bring enormous benefits to attosecond science, too.

### Acknowledgements

This work was supported by the Hungarian Scientific Research Fund (OTKA No. T048324), the FWF Austria (grants F016, P15382 and Z63) and the ULTRA COST P14 Action of the EU. P.D. acknowledges support from the Hungarian State Eötvös Fellowship.

### References

- [1] T. Brabec and F. Krausz, *Rev. Mod. Phys.* **72** 545 (2000).
- [2] P. Agostini and L. DiMauro, *Rep. Prog. Phys.* **67** 813 (2004).
- [3] P. Dombi, A. Apolonski, Ch. Lemell, *et al.*, *New J. Phys.* **6** 39 (2004).
- [4] Ch. Lemell, X.-M. Tong, F. Krausz, *et al.*, *Phys. Rev. Lett.* **90** 076403 (2003).
- [5] A. Apolonski, P. Dombi, G.G. Paulus, *et al.*, *Phys. Rev. Lett.* **92** 073902 (2004).
- [6] R. Srinivasan, V.A. Lobastov, C.-Y. Ruan, *Helv. Chim. Acta* **86** 1761 (2003).
- [7] S.E. Irvine, A. Dechant and A.Y. Elezzabi, *Phys. Rev. Lett.* **93** 184801 (2004).
- [8] H. Petek and S. Ogawa, *Prog. Surf. Sci.* **56** 239 (1997).
- [9] M. Weinelt, *J. Phys. Cond. Mat.* **14** R1099 (2002).
- [10] G.H. Fecher, O. Schmidt, Y. Hwu, *et al.*, *J. Electron Spectrosc.* **126** 77 (2002).
- [11] T. Munakata, T. Masuda, N. Ueno, *et al.*, *Surf. Sci.* **507** 434 (2002).
- [12] K. Ishioka, C. Gahl and M. Wolf, *Surf. Sci.* **454** 73 (2000).
- [13] P.B. Corkum, *Phys. Rev. Lett.* **71** 1994 (1993).
- [14] M. Lewenstein, P. Balcou, M.Y. Ivanov, *et al.*, *Phys. Rev. A* **49** 2117 (1994).
- [15] F.W. Helbing, G. Steinmeyer and U. Keller, *Laser Phys.* **13** 644 (2002).
- [16] S. Sartania, Z. Cheng, M. Lenzner, *et al.*, *Opt. Lett.* **22** 1562 (1997).
- [17] U. Schwengelbeck, L. Plaja, E.C. Jarque, *et al.*, *J. Phys. B* **35** L181 (2002).
- [18] T. Hattori, Y. Kawashima, M. Daikoku, *et al.*, *Jpn. J. Appl. Phys.* **39** 4793 (2000).
- [19] M.J. Weida, S. Ogawa, H. Nagano, *et al.*, *J. Opt. Soc. Am. B* **17** 1443 (2000).
- [20] J. Cao, Y. Gao, H.E. Elsayed-Ali, *et al.*, *Phys. Rev. B* **58** 1948 (1998).
- [21] M. Aeschlimann, M. Bauer, S. Pawlik, *et al.*, *Appl. Phys. A* **71** 485 (2000).
- [22] A.T. Georges, *Phys. Rev. B* **51** 13735 (1995).
- [23] A.T. Georges, *Phys. Rev. A* **54** 2412 (1996).
- [24] F.H.M. Faisal and J.Z. Kaminski, *Phys. Rev. A* **56** 748 (1997).
- [25] F.H.M. Faisal and J.Z. Kaminski, *Phys. Rev. A* **58** R19 (1998).
- [26] I. Campillo, J.M. Pitarke, A. Rubio, *Phys. Rev. B* **62** 1500 (2000).